Interacting Chern Insulator in Infinite Spatial Dimensions

David Krüger[1] and Michael Potthoff[1,2]
[1]I. Institute of Theoretical Physics, Department of Physics, University of Hamburg, Notkestraße 9-11, 22607 Hamburg, Germany
[2]The Hamburg Centre for Ultrafast Imaging, Luruper Chaussee 149, 22761 Hamburg, Germany

(Received 15 September 2020; accepted 13 April 2021; published 10 May 2021)

We study a generic model of a Chern insulator supplemented by a Hubbard interaction in arbitrary even dimension D and demonstrate that the model remains well defined and nontrivial in the $D \to \infty$ limit. Dynamical mean-field theory is applicable and predicts a phase diagram with a *continuum* of topologically different phases separating a correlated Mott insulator from the trivial band insulator. We discuss various features, such as the elusive distinction between insulating and semimetal states, which are unconventional already in the noninteracting case. Topological phases are characterized by a nonquantized Chern *density* replacing the Chern number as $D \to \infty$.

DOI: 10.1103/PhysRevLett.126.196401

Introduction.—Strong electron correlations and topological classification are two major research frontiers of condensed-matter theory. While much work has been done in providing prototypical examples of topologically nontrivial quantum matter [1–4] and in classifying [5–9] topological insulators, much less is known for correlated systems [10–13]. As correlated lattice-fermion models in $D = 2$ and $D = 3$ dimensions pose highly involved problems, many studies focus on one-dimensional systems with nontrivial topological properties [14–20].

On the other hand, the opposite limit of infinite spatial dimensions has been recognized as extremely instructive for the pure electron-correlation problem and constitutive for the dynamical mean-field theory (DMFT) [21]. In the large class of mean-field approaches, DMFT has an exceptional standing, since it is internally consistent and nonperturbative, and since it becomes exact in the $D \to \infty$ limit [22]. While the limit comes with certain simplifications, such as the locality of the self-energy [21,23], infinite-dimensional lattice-fermion models are far from being trivial. This is demonstrated by the DMFT paradigm of the Mott metal-insulator transition as a prime example [24]. Furthermore, the fact that exact properties of strongly correlated systems are numerically accessible [21,25,26], make correlated lattice-fermion models on $D = \infty$ lattices attractive points of orientation.

With the present study we pose the question whether the same limit is also helpful for the understanding of topological properties of strongly interacting electron systems. Our answer is affirmative. Assuming locality of the self-energy, previous DMFT studies of correlated topological insulators have addressed two-dimensional systems, such as the Haldane model [27], Hofstadter's butterfly [28], or the Bernevig-Hughes-Zhang model [29,30], all supplemented by interaction terms, or real three-dimensional systems, such as SmB_6 [31], combining the DMFT with *ab initio* band theory. A DMFT study of an interacting, topologically nontrivial model on a $D = \infty$ lattice is still missing.

Here, we consider multiorbital Hubbard models on a D-dimensional hypercubic lattice for arbitrary but even D, whose low-energy noninteracting band structures reduce to massive Dirac theories and belong to class A of Chern insulators with $\mathbb{Z}$ topological invariants. We demonstrate that, with the proper scaling of the hopping, the $D \to \infty$ limit leads to a well-defined model with nontrivial interplay between kinetic and interaction terms, hosting topologically nontrivial phases, and is accessible to a numerical solution by DMFT for arbitrary Hubbard interaction U and mass parameter m. The m-U phase diagram contains the trivial band and the correlated Mott insulator, separated by a *continuum* of interacting and topologically different Chern insulators. The latter are characterized by a properly defined Chern *density*, which replaces the Chern number as a topological invariant. We argue that for $D \to \infty$ already the $U = 0$ model has highly unconventional topological properties since the sign of the Chern number as well as a band closure are concepts becoming ill defined in the limit $D \to \infty$.

Hamiltonian.—We study an extension of a family of D-dimensional tight-binding models for even D to spinful fermions with local Coulomb interaction as described by the Hamiltonian $H = H_0 + H_1$. Here, $H_1 = (U/2)\sum_{i\alpha\sigma} n_{i\alpha\sigma} n_{i\alpha-\sigma}$ is an on-site and intraorbital Hubbard term, where $i = 1, \ldots, L$ labels the sites of a D-dimensional hypercubic lattice with periodic boundaries, $\sigma = \uparrow, \downarrow$ is the spin projection, and $\alpha = 1, \ldots, M$ is an orbital index. The corresponding annihilator is $c_{i\alpha\sigma}$, and $n_{i\alpha\sigma} \equiv c^\dagger_{i\alpha\sigma} c_{i\alpha\sigma}$. After Fourier transformation to k space, $c_{i\alpha\sigma} = L^{-1/2} \sum_k e^{ikR_i} c_{k\alpha\sigma}$, the tight-binding part reads $H_0 = \sum_{k\alpha\beta\sigma} \epsilon_{\alpha\beta}(k) c^\dagger_{k\alpha\sigma} c_{k\beta\sigma}$, where $k = (k_1, \ldots, k_D)$

with $-\pi < k_r \leq \pi$, and where $\epsilon_{\alpha\beta}(k)$ are the elements of the $M \times M$ hopping matrix in k space:

$$\boldsymbol{\epsilon}(k) = \left(m + t\sum_{r=1}^{D}\cos k_r\right)\boldsymbol{\gamma}_D^{(0)} + t\sum_{r=1}^{D}\sin k_r\boldsymbol{\gamma}_D^{(r)}, \quad (1)$$

depending on the hopping parameter t and on a parameter m controlling the mass term. Here, $\boldsymbol{\gamma}_D^{(1)}, \ldots, \boldsymbol{\gamma}_D^{(D)}$ are the generators of the complex Clifford algebra $\mathbb{C}l_D$, and $\boldsymbol{\gamma}_D^{(0)} = (-i)^{D/2}\boldsymbol{\gamma}_D^{(1)}\cdots\boldsymbol{\gamma}_D^{(D)}$ is the chiral element. They satisfy the Clifford anticommutation relations $\{\boldsymbol{\gamma}_D^{(\mu)}, \boldsymbol{\gamma}_D^{(\nu)}\} = 2\delta^{(\mu\nu)}$ for $\mu, \nu = 0, 1, \ldots, D$. Close to the critical points k_c in the first Brillouin zone (BZ), see below, the low-energy effective theory is given by a linear Dirac model with k-independent mass term. Such free Dirac models are extensively analyzed and topologically classified for different mass terms and for arbitrary D, see e.g., Ref. [32]. The model (1) belongs to symmetry class A in the Altland-Zirnbauer (AZ) scheme [6].

We note that $\mathbb{C}l_{D+2} \cong \mathrm{Mat}(2, \mathbb{C}) \otimes \mathbb{C}l_D$ and that there is, for even D, a unique irreducible $M = 2^{D/2}$-dimensional matrix representation of $\mathbb{C}l_D$ [33–35]. The according $\boldsymbol{\gamma}$ matrices can be constructed recursively: $\mathbb{C}l_0$ is spanned by $1 \in \mathbb{C}$. The first nontrivial dimension is $D = 2$, and hence $M = 2$. $\mathbb{C}l_2$ is generated by the Pauli matrices $\boldsymbol{\gamma}_2^{(1)} = \boldsymbol{\tau}_x$ and $\boldsymbol{\gamma}_2^{(2)} = \boldsymbol{\tau}_y$, and together with the unity $\mathbf{1}$ and the chiral element $\boldsymbol{\gamma}_2^{(0)} = -i\boldsymbol{\tau}_x\boldsymbol{\tau}_y = \boldsymbol{\tau}_z$, they span $\mathbb{C}l_2$. The corresponding generalized lattice Dirac model, Eq. (1), with $\boldsymbol{\epsilon}(k) = d(k)\cdot\boldsymbol{\tau}$ and $d(k) = (t\sin k_x, t\sin k_y, m + t\cos k_x + t\cos k_y)$ is just the model proposed by Qi, Wu, and Zhang [36,37]. For arbitrary even D the general recursive prescription for the Hermitian and traceless generators is [32]:

$$\begin{aligned}\boldsymbol{\gamma}_{D+2}^{(r)} &= \boldsymbol{\tau}_x \otimes \boldsymbol{\gamma}_D^{(r)} \quad \text{for } r = 1, \ldots, D,\\ \boldsymbol{\gamma}_{D+2}^{(D+1)} &= \boldsymbol{\tau}_x \otimes \boldsymbol{\gamma}_D^{(0)}, \qquad \boldsymbol{\gamma}_{D+2}^{(D+2)} = \boldsymbol{\tau}_y \otimes \mathbf{1}. \end{aligned} \quad (2)$$

The chiral element is $\boldsymbol{\gamma}_{D+2}^{(0)} = \boldsymbol{\tau}_z \otimes \mathbf{1}$, where $\mathbf{1}$ denotes the $2^{D/2}$-dimensional unity. Explicitly, $\boldsymbol{\gamma}^{(0)} = \mathrm{diag}(+1, +1, \ldots, -1, -1, \ldots)$, such that m is the strength of a staggered on-site potential in Eq. (1). Accordingly, the orbitals α can be divided into two classes, A orbitals with $\gamma_{\alpha\alpha}^{(0)} \equiv z_\alpha = +1$ $(\alpha = 1, \ldots, M/2)$ and B orbitals $\gamma_{\alpha\alpha}^{(0)} \equiv z_\alpha = -1$ $[\alpha = (M/2) + 1, \ldots, M]$. We see that the number of orbitals scales exponentially with D. Equations (1) and (2) imply that along a spatial direction r, each site-orbital (i, α) couples to a single orbital α' at the two nearest-neighbor positions i', and thus the connectivity of (i, α) is $2D$.

Noninteracting case.—The $U = 0$ band structure is easily obtained by squaring $\boldsymbol{\epsilon}(k)$, using properties of the $\boldsymbol{\gamma}$ matrices, and noting that $\mathrm{tr}\boldsymbol{\epsilon}(k) = 0$. Apart from the spin degeneracy, this yields two $M/2$-fold degenerate bands: $\epsilon_\pm(k) = \pm[t^2\sum_r \sin^2 k_r + (m + t\sum_r \cos k_r)^2]^{1/2}$. The high-energy band edges are given by $\epsilon_{\mathrm{max,min}} = \pm(|m| + Dt)$ and are taken for $k_r = 0$ (if $m \geq 0$) and $k_r = \pi$ $(m \leq 0)$ for all r. Because of the point-group symmetries, band closures are found at the high-symmetry points (HSPs) $k_c = k_{n_0} = (0, \ldots, 0, \pi, \ldots, \pi)$ in the BZ, and for $\binom{D}{n_0}$ inequivalent permutations of the components, where n_0 counts the number of vanishing entries k_r. For a band closure the condition $m = (D - 2n_0)t$ must be met. This corresponds to the vanishing of the mass term in the Dirac Hamiltonian $\boldsymbol{\epsilon}(k) = [m + (2n_0 - D)t]\boldsymbol{\gamma}_D^{(0)} + t\sum_r (k_r - k_{n_0,r})\boldsymbol{\gamma}_D^{(r)}$, obtained by linearization of $\boldsymbol{\epsilon}(k)$ around k_{n_0}.

Infinite dimensions.—It is instructive to compute the low-order moments $M_\alpha^{(n)} = \int d\omega \rho_\alpha^n(\omega)$ of the local partial density of states (DOS) of the orbital α. We have the trivial normalization condition $M_\alpha^{(0)} = 1$, the barycenter $M_\alpha^{(1)} = m\gamma_{\alpha\alpha}^{(0)} = \pm m$, and the α-independent second moment $M_\alpha^{(2)} = t^2 D + m^2$. The variance of the DOS is given by the second central moment $M_\alpha^{(2)} - (M_\alpha^{(1)})^2 = t^2 D$. Hence, a proper $D \to \infty$ limit with a balance between H_0 and H_1 is obtained if the standard [22,38] scaling $t = t^*/\sqrt{D}$ with lattice dimension D is employed. This will be assumed here as well. Furthermore, we fix the energy scale by setting $t^* = 1$, i.e., the variance of the DOS is unity, while the locations of the band edges diverge $\epsilon_{\mathrm{max,min}} = \pm(|m| + \sqrt{D}t^*) \mapsto \pm\infty$. The mass parameter m must not be scaled in the $D \to \infty$ limit to maintain a nontrivial model. This implies a D-independent band center of gravity $\pm m$.

Topology for $D \to \infty$.—We approach the $D \to \infty$ limit via even-D models of Chern insulators and stay in the AZ class A. For any finite even D, upon varying m, one passes band closures and related topological phase transitions, located at $m = \sqrt{D}(1 - 2n_0/D)t^*$ for $n_0 = 0, \ldots, D$. Figure 1 (left) gives an example for $D = 4$. The topological phase for an m with $D - 2n_0 - 2 < m\sqrt{D}/t^* < D - 2n_0$ (with $n_0 = 0, \ldots, D - 1$) can be characterized by the $(D/2)$th Chern number [32,39,40]:

$$C_D(n_0) = (-1)^{n_0 + (D/2)}\binom{D-1}{n_0}, \quad (3)$$

see Fig. 1 (middle) for an overview. The equation can be interpreted by referring to the bulk-boundary correspondence [7]. Namely, the $(D - 1)$-dimensional surface characterized by Miller indices $(100\ldots0)$ hosts topologically protected surface states, and their dispersion has Weyl nodes at the surface projections $k_{c,\parallel}$ of the bulk HSPs k_c for given n_0. The binomial factor in Eq. (3) counts the number of equivalent nodal $k_{c,\parallel}$ points in the $(D - 1)$-dimensional

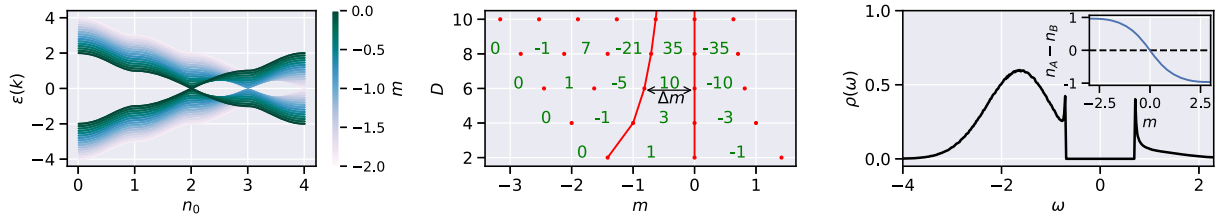

FIG. 1. Left: band structure $\epsilon(k) = \epsilon_{\pm}(k)$ of the $D = 4$ model along straight shortest lines in the BZ connecting HSPs characterized by n_0. Results for different m, see color code. Middle: different topological phases with Chern numbers $C_D(n_0)$ (green), separated by critical m values (red dots) for different D. Right: $U = 0$ DOS on the A orbitals at $m = -1.5$ for $D = \infty$. Inset: orbital polarization as function of m for $D = \infty$. Nearest-neighbor hopping: $t = t^*/\sqrt{D}$, $t^* = 1$ sets the energy scale.

surface Brillouin zone. All Weyl points have the same chirality given by the sign factor [32].

Importantly, the distance between two transitions $\Delta m = 2t^*/\sqrt{D}$ shrinks to zero for $D \to \infty$, i.e., the set of critical m's becomes dense in any finite m interval. Hence, for high D the system is arbitrarily close to criticality for *any* m. We note that, mathematically, the definition of a critical point in the BZ becomes elusive for $D \to \infty$, since $\epsilon_{\pm}(k) = \epsilon_{\pm}(k')$ if $\|k - k'\| = 0$, where we have defined $\|k\|^2 \equiv \lim_{D\to\infty} D^{-1} \sum_{r=1}^{D} k_r^2$. It is easy to see that $\|\cdot\|$ is a seminorm, i.e., $\|k\| = 0 \not\Rightarrow k = 0$, such that the concept of a band closure at isolated points in k space breaks down. However, we still have $\epsilon_{\pm}(k) = 0$ at $k = k_c(m)$ for any m. Furthermore, the number $\binom{D}{n_0}$ of equivalent critical HSPs at a given critical m and the total number 2^D of HSPs in the BZ diverge, but their ratio approaches a constant when $D \to \infty$.

A second important observation directly follows from Eq. (3): When $D \to \infty$, only the *modulus* of the Chern number, and only after proper *normalization*, has a well-defined limit. Noting that $\sum_{n_0=0}^{D-1} C_D(n_0) = 2^{D-1}$, we thus introduce a Chern density as $c(n_0) = \lim_{D\to\infty} |C_D(n_0)|/2^{D-1}$. Since $\Delta m \mapsto 0$, we can use $n_0 = (D - m\sqrt{D}/t^*)/2$ and $dm \equiv 2t^*/\sqrt{D}$ to express the Chern density as a function of m. With this, and using the Moivre-Laplace theorem, we find

$$c(n_0) = \lim_{D\to\infty} \sqrt{\frac{2}{\pi D}} e^{-2[(D/2)-n_0]^2/D} = c(m)dm \quad (4)$$

with a normalized Chern density of unit variance:

$$c(m) = \frac{1}{t^*\sqrt{2\pi}} e^{-m^2/2t^{*2}}. \quad (5)$$

This is a central result, as it shows that not only dynamic correlation effects but also nontrivial topological properties survive the $D \to \infty$ limit when using the standard scaling of the hopping.

From the bulk-boundary correspondence [7,32,41] at any finite D, we can infer that $c(m)dm$ is the ratio between the number of topologically protected surface states and the total number of HSPs in the BZ. Upon variation of $m \mapsto m + dm$, a ratio of $\pm 2c(m)dm$ bulk states (per total number of HSPs) traverse the gap at the HSPs corresponding to m. The Chern density is insensitive to the sign though.

Density of states.—Turning to the correlation side of the problem, the relevant quantity for the DMFT is the $U = 0$-DOS $\rho_\alpha(\omega) = -(1/\pi L)\mathrm{Im}\sum_k G^{(0)}_{\alpha\alpha}(k, \omega + i0^+)$ of orbital α. This can be computed efficiently using the quasi–Monte Carlo technique of Refs. [42,43] to carry out the k summation. Thanks to the Clifford algebra, the inversion of the $M \times M$ hopping matrix required to get the noninteracting Green's function matrix $\boldsymbol{G}^{(0)}_{\boldsymbol{k}}(\omega) = 1/[\omega - \epsilon(\boldsymbol{k})]$ can be done analytically, see Sec. A of the Supplemental Material (SM) [44]. We also derive an analytical expression for the DOS in the $D \to \infty$ limit (SM, Sec. B [44]). For any D, we have $\rho_A(-\omega) = \rho_B(\omega)$, and for $m \mapsto -m$, the DOS transforms as $\rho_\alpha(\omega) \mapsto \rho_\alpha(-\omega)$. The $D = \infty$ DOS is shown in Fig. 1 (right).

Another important point is that the $D = \infty$ DOS is fully gapped *for all* m. Furthermore, the gap $\Delta = \sqrt{2}t^*$ is m independent. This should be contrasted with the DOS at any finite D, which behaves at low frequencies and at a critical m as $\rho_\alpha(\omega) \propto |\omega|^{D-1}$, as it is characteristic for a Dirac-cone structure (SM, Sec. C [44]). The band states near a band closure in k space at a critical k_c and all equivalent points (including k points with $\|k - k_c\| = 0$) do no longer contribute a finite DOS near $\omega = 0$. Hence, there is no meaningful distinction between insulator and semimetal states in the $D \to \infty$ limit.

The relevant range of the mass parameter to get nontrivial correlation effects in high D is of order $m = \pm\mathcal{O}(t^*)$. This is demonstrated with the inset of Fig. 1 (right) showing the orbital polarization $p = (n_A - n_B)/2$ of the half-filled noninteracting system, $(n_A + n_B)/2 = 1$, as a function of m (where $n_\alpha \equiv L^{-1}\sum_{k\sigma}\langle c^\dagger_{k\alpha\sigma} c_{k\alpha\sigma}\rangle$). On the scale $m = \pm\mathcal{O}(t^*)$, p quickly approaches almost full saturation with empty or doubly occupied A (or B) orbitals, i.e., a state where the Hubbard interaction is static and correlation effects are absent.

DMFT.—The exact solution of the interacting model in the $D \to \infty$ limit is provided by the DMFT. Particularly, the

m-U phase diagram of the model is interesting as it expresses the generic interplay of topological properties *and* correlations in an exactly solvable and nonperturbative case. To cover the entire relevant parameter space, we employ a simplified DMFT scheme, where the interacting lattice model is self-consistently mapped onto a two-site single-impurity Anderson model [45]. A slight generalization is necessary to account for the A-B orbital structure. This generalized two-site DMFT (see SM, Secs. D and E for details [44]) simultaneously focuses on the low- and on the high-frequency limit of the DMFT self-consistency condition and qualitatively captures the Mott-transition physics [45–47].

At finite U the $(D/2)$th Chern number can be expressed in terms of the interacting single-particle Green's function [48–50]. Here, for $D \to \infty$, the locality of the self-energy allows us to apply the concept of the topological Hamiltonian [50] (see also Ref. [51]) and to compute $c(m)$ from the noninteracting part but with $\boldsymbol{\epsilon}(k) \mapsto \boldsymbol{\epsilon}(k) - \mu\mathbf{1} + \mathbf{\Sigma}(\omega = 0)$ and where the chemical potential $\mu = U/2$. Since $\mathbf{\Sigma}(\omega)$ is diagonal in orbital space (see SM, Sec. D [44]), this merely amounts to a renormalization of the chemical potential, $\mu \mapsto \mu + \Sigma_+(\omega = 0)$, and the mass parameter, $m \mapsto m + \Sigma_-(\omega = 0)$, where $\Sigma_\pm(\omega) = (\Sigma_A(\omega) \pm \Sigma_B(\omega))/2$. For finite D we have successfully tested our results case by case against the predictions of the pole-expansion technique [29,31,52], which applies if the self-energy is given in its discrete Lehmann representation [53].

Phase diagram.—We have performed DMFT calculations, restricted to spin-symmetric states in a large range of parameters m and U. The resulting Chern density $c(m, U)$ is shown in Fig. 2. As the phase diagram is invariant under a sign change $m \mapsto -m$, only negative m values are displayed. At $U = 0$ and as a function of m, the Chern density is a Gaussian, see Eq. (5), and the system smoothly evolves from a conventional band insulator, with $c(m, 0) \to 0$ in the limit $m \to -\infty$, to a Chern insulator-semimetal with a maximum $c(m, 0) = 1/\sqrt{2\pi}$ at the symmetric point $m = 0$.

With increasing U at $m = 0$, the Chern density $c(0, U)$ stays at its maximum until at $U = U_c = 6t^*$, the system undergoes a correlation-driven transition to a topologically trivial Mott phase with $c = 0$. With a refined DMFT scheme only a slightly lower U_c is expected [45]. Approaching U_c either from above or from below, the transition is characterized by a continuously vanishing renormalization factor $z \mapsto 0$, where $z \equiv 1/[1 - \partial\Sigma_\alpha(\omega = 0)/\partial\omega]$ is independent of the orbital type α. z plays the role of a band-gap renormalization [54].

The Mott phase extends to $m < 0$ and is bounded for all m by a line of critical interactions $U_c(m)$. For $m \to -\infty$ we observe that $U_c(m)$ linearly increases with $|m|$. This is explained by the fact that the system becomes fully orbital polarized. Hence, the self-energy becomes static and approaches constants $\Sigma_A \to U$, $\Sigma_B \to 0$, such that the renormalization of m is trivial: $m \to m + \Sigma_-(\omega = 0) \to m + U/2$. As a consequence, the band insulator with $c = 0$ cannot be smoothly connected to the Mott insulator with $c = 0$ without passing topologically nontrivial states with $c > 0$.

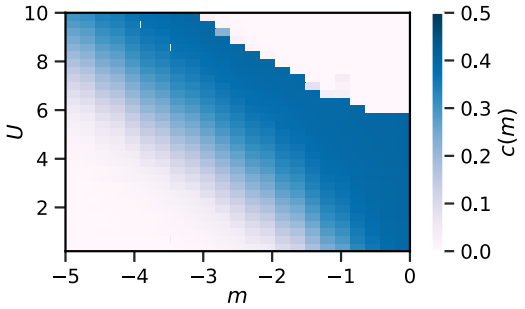

FIG. 2. m-U phase diagram of the $D \to \infty$ model. The color codes the Chern density.

The whole phase diagram can be understood as the $D \to \infty$ limit of m-U phase diagrams at finite D, see SM, Sec. F [44]. With increasing D, the number of topologically nontrivial phases $C_D(m) \neq 0$ increases and become ever narrower regions in the m-U plane, until they shrink to one-dimensional lines (of constant color in Fig. 2) given by $c(m, U) = \text{const}$. This implies that, in the limit $D \to \infty$, systems on these iso-Chern curves are topologically equivalent, while on paths crossing iso-Cherns one passes through a continuum of topologically different phases.

Conclusions and outlook.—DMFT is nowadays mostly employed as an approximate approach to strongly correlated lattice-fermion models in low dimensions. The fact that DMFT becomes exact in the $D \to \infty$, however, is a central aspect of the approach, as it ensures its internal consistency in the entire parameter space spanned by hopping, interaction, filling, orbital hybridization, and more. It is thus important to demonstrate the very existence of an infinite-dimensional interacting lattice model with nontrivial topological properties that is in fact exactly solved by the DMFT. The generic model of an interacting Chern insulator studied here is the first example of this kind.

Our approach has shown that with the conventional scaling of the hopping parameter, a nontrivial interplay between strong local correlations and topological properties is retained in the $D \to \infty$ limit and thus paves the way for further *generic* studies of this and of other models, including models in different AZ classes. Such studies offer the unique possibility to exactly access intertwined correlation and topological effects in a nonperturbative regime and support approximate DMFT studies of low-D cases. They furthermore disentangle the pure and generic (dynamical) mean-field content of the theory from the additional realistic features of the DMFT when applied to low-D models with specific lattice and orbital structure. Clearly, also controlled "expansions" around the $D \to \infty$ limit, using cluster or diagrammatic schemes, profit from a

well-defined and nontrivial starting point, e.g., for benchmarking.

The question of what is generic and what is specific in the context of interacting mean-field theory can also be posed with respect to the topological invariant itself. For the model studied here, there is a continuum of topologically different phases, characterized by a Chern density, which is a smooth, nonquantized function of m and U, except at the Mott transition. Importantly, one can further elaborate on these ideas already in $U = 0$ limit. While this provokes the question of whether analogs can be found in finite-D models, these features are interesting in themselves and one may even speculate about a possibly different topological classification in the $D \to \infty$ limit.

At the fundamental level of topological classification, there is obviously a plethora of open questions, including the robustness against including interactions [55], relevance of periodicity in the spatial dimension for interacting systems [56], etc. Furthermore, we note that there are other routes to topological phases as well: Nontrivial topological states could be generated by starting from a topologically trivial model in the $D \to \infty$ limit, either at some finite D or via extensions of DMFT. Exact statements or even the exact construction of entire phase diagrams and of excitations spectra, however, are probably difficult to achieve beyond the dynamical mean-field concept but highly desirable.

This work was supported by the Deutsche Forschungsgemeinschaft (DFG) through the Cluster of Excellence "Advanced Imaging of Matter"–EXC 2056–project ID 390715994, and by the DFG Sonderforschungsbereich 925 "Light-induced dynamics and control of correlated quantum systems" (project B5).

[1] M. Z. Hasan and C. L. Kane, Rev. Mod. Phys. **82**, 3045 (2010).
[2] X.-L. Qi and S.-C. Zhang, Rev. Mod. Phys. **83**, 1057 (2011).
[3] D. J. Thouless, M. Kohmoto, M. P. Nightingale, and M. den Nijs, Phys. Rev. Lett. **49**, 405 (1982).
[4] K. von Klitzing, Rev. Mod. Phys. **58**, 519 (1986).
[5] M. R. Zirnbauer, J. Math. Phys. (N.Y.) **37**, 4986 (1996).
[6] A. Altland and M. R. Zirnbauer, Phys. Rev. B **55**, 1142 (1997).
[7] A. P. Schnyder, S. Ryu, A. Furusaki, and A. W. W. Ludwig, Phys. Rev. B **78**, 195125 (2008).
[8] T. Morimoto and A. Furusaki, Phys. Rev. B **88**, 125129 (2013).
[9] C.-K. Chiu, J. C. Y. Teo, A. P. Schnyder, and S. Ryu, Rev. Mod. Phys. **88**, 035005 (2016).
[10] L. Fidkowski and A. Kitaev, Phys. Rev. B **81**, 134509 (2010).
[11] M. Hohenadler, T. C. Lang, and F. F. Assaad, Phys. Rev. Lett. **106**, 100403 (2011).
[12] T. Yoshida, R. Peters, S. Fujimoto, and N. Kawakami, Phys. Rev. Lett. **112**, 196404 (2014).
[13] S. Rachel, Rep. Prog. Phys. **81**, 116501 (2018).
[14] A. M. Turner, F. Pollmann, and E. Berg, Phys. Rev. B **83**, 075102 (2011).
[15] H. Guo and S.-Q. Shen, Phys. Rev. B **84**, 195107 (2011).
[16] S. R. Manmana, A. M. Essin, R. M. Noack, and V. Gurarie, Phys. Rev. B **86**, 205119 (2012).
[17] F. Grusdt, M. Höning, and M. Fleischhauer, Phys. Rev. Lett. **110**, 260405 (2013).
[18] J. Sirker, M. Maiti, N. P. Konstantinidis, and N. Sedlmayr, J. Stat. Mech. (2014) P10032.
[19] A. Hayward, C. Schweizer, M. Lohse, M. Aidelsburger, and F. Heidrich-Meisner, Phys. Rev. B **98**, 245148 (2018).
[20] M. Schmitt and S. Kehrein, Phys. Rev. B **98**, 180301(R) (2018).
[21] A. Georges, G. Kotliar, W. Krauth, and M. J. Rozenberg, Rev. Mod. Phys. **68**, 13 (1996).
[22] W. Metzner and D. Vollhardt, Phys. Rev. Lett. **62**, 324 (1989).
[23] E. Müller-Hartmann, Int. J. Mod. Phys. B **03**, 2169 (1989).
[24] F. Gebhard, *The Mott Metal-Insulator Transition* (Springer, Berlin, 1997).
[25] E. Gull, A. J. Millis, A. Lichtenstein, A. N. Rubtsov, M. Troyer, and P. Werner, Rev. Mod. Phys. **83**, 349 (2011).
[26] Y. Lu, M. Höppner, O. Gunnarsson, and M. W. Haverkort, Phys. Rev. B **90**, 085102 (2014).
[27] T. I. Vanhala, T. Siro, L. Liang, M. Troyer, A. Harju, and P. Törmä, Phys. Rev. Lett. **116**, 225305 (2016).
[28] A. A. Markov, G. Rohringer, and A. N. Rubtsov, Phys. Rev. B **100**, 115102 (2019).
[29] L. Wang, H. Jiang, X. Dai, and X. C. Xie, Phys. Rev. B **85**, 235135 (2012).
[30] A. Amaricci, J. C. Budich, M. Capone, B. Trauzettel, and G. Sangiovanni, Phys. Rev. Lett. **114**, 185701 (2015).
[31] P. Thunström and K. Held, arXiv:1907.03899.
[32] E. Prodan and H. Schulz-Baldes, *Bulk and Boundary Invariants for Complex Topological Insulators: From K-Theory to Physics* (Springer, New York, 2016).
[33] S. Lang, *Algebra* (Springer, New York, 2002).
[34] M. R. de Traubenberg, arXiv:hep-th/0506011.
[35] A. H. Bilge, S. Kocak, and S. Uguz, Linear Algebra Appl. **419**, 417 (2006).
[36] X.-L. Qi, Y.-S. Wu, and S.-C. Zhang, Phys. Rev. B **74**, 085308 (2006).
[37] J. Asbóth, L. Oroszlány, and A. Pályi, *The Su-Schrieffer-Heeger (SSH) Model*, A Short Course on Topological Insulators. Lecture Notes in Physics Vol. 919 (Springer, Cham, 2016).
[38] E. Müller-Hartmann, Z. Phys. B **74**, 507 (1989).
[39] M. F. L. Golterman, K. Jansen, and D. B. Kaplan, Phys. Lett. B **301**, 219 (1993).
[40] X.-L. Qi, T. L. Hughes, and S.-C.Zhang, Phys. Rev. B **78**, 195424 (2008).
[41] A. M. Essin and V. Gurarie, Phys. Rev. B **84**, 125132 (2011).
[42] F. Y. Kuo and D. Nuyens, Found. Comput. Math. **16**, 1631 (2016).
[43] P. L'Ecuyer, in *Proceedings of the 12th International Conference on Monte Carlo and Quasi-Monte Carlo Methods in Scientific Computing (MCQMC 2016), Stanford, CA* (Springer, Cham, 2016), https://link.springer.com/book/10.1007/978-3-319-91436-7.

[44] See Supplemental Material at http://link.aps.org/supplemental/10.1103/PhysRevLett.126.196401 for various technical details and supplemental numerical results.
[45] M. Potthoff, Phys. Rev. B **64**, 165114 (2001).
[46] R. Bulla and M. Potthoff, Eur. Phys. J. B **13**, 257 (2000).
[47] S. Schwieger, M. Potthoff, and W. Nolting, Phys. Rev. B **67**, 165408 (2003).
[48] K. Ishikawa and T. Matsuyama, Z. Phys. C **33**, 41 (1986).
[49] Z. Wang, X.-L. Qi, and S.-C. Zhang, Phys. Rev. Lett. **105**, 256803 (2010).
[50] Z. Wang and S.-C. Zhang, Phys. Rev. X **2**, 031008 (2012).
[51] Y.-Y. He, H.-Q. Wu, Z. Y. Meng, and Z.-Y. Lu, Phys. Rev. B **93**, 195164 (2016).
[52] S. Y. Savrasov, K. Haule, and G. Kotliar, Phys. Rev. Lett. **96**, 036404 (2006).
[53] C. Gramsch and M. Potthoff, Phys. Rev. B **92**, 235135 (2015).
[54] M. Sentef, J. Kuneš, P. Werner, and A. P. Kampf, Phys. Rev. B **80**, 155116 (2009).
[55] L. Fidkowski and A. Kitaev, Phys. Rev. B **83**, 075103 (2011).
[56] D. Gaiotto and T. Johnson-Freyd, J. High Energy Phys. 2019 (2019) 7.